TISSUE ENGINEERING: Part A
Volume 15, Number 3, 2009

DOI: 10.1089/ten.tea.2008.0196

Micropatterning of Poly(Ethylene Glycol) Diacrylate Hydrogels with Biomolecules to Regulate and Guide Endothelial Morphogenesis

James J. Moon, Ph.D., Mariah S. Hahn, Ph.D., Iris Kim, B.S., Barbara A. Nsiah, B.S., and Jennifer L. West, Ph.D.

Angiogenesis, which is morphogenesis undertaken by endothelial cells (ECs) during new blood vessel formation, has been traditionally studied on natural extracellular matrix proteins. In this work, we aimed to regulate and guide angiogenesis on synthetic, bioactive poly(ethylene glycol)-diacrylate (PEGDA) hydrogels. PEGDA hydrogel is intrinsically cell nonadhesive and highly resistant to protein adsorption, allowing a high degree of control over presentation of ligands for cell adhesion and signaling. Since these materials are photopolymerizable, a variety of photolithographic technologies may be applied to spatially control presentation of bioactive ligands. To manipulate EC adhesion, migration, and tubulogenesis, the surface of PEGDA hydrogels was micropatterned with a cell adhesive ligand, Arg-Gly-Asp-Ser (RGDS), in desired concentrations and geometries. ECs cultured on these RGDS patterns reorganized their cell bodies into cord-like structures on 50-μm-wide stripes, but not on wider stripes, suggesting that EC morphogenesis can be regulated by geometrical cues. The cords formed by ECs were reminiscent of capillaries with cells participating in the self-assembly and reorganization into multicellular structures. Further, endothelial cord formation was stimulated on intermediate concentration of RGDS at 20 $\mu g/cm^2$, whereas it was inhibited at higher concentrations. This work has shown that angiogenic responses can be tightly regulated and guided by micropatterning of bioactive ligands and also demonstrated great potentials of micropatterned PEGDA hydrogels for various applications in tissue engineering, where vascularization prior to implantation is critical.

Introduction

The formation of blood vessels is essential for establishment and maintenance of tissues. Angiogenesis refers to the formation of new capillary blood vessels by a process of sprouting from preexisting vessels and is often studied *in vitro* by stimulating monolayers of endothelial cells (ECs) to assemble into sprouts or tubes.[1] This complex process of new blood vessel formation is orchestrated by interplay between ECs and their neighboring mural cells via various cytokines, extracellular matrix (ECM) proteins, integrins, and proteases.[2] Ever since the introduction of the *in vitro* model of angiogenesis,[3] there have been great research interest to understand the intricate process of angiogenesis; however, the details of conditions that govern angiogenesis are yet to be delineated.

Natural ECMs have been used widely in blood vessel biology research due to their ease of preparation and manipulation. For examination of angiogenesis on two-dimensional (2D) surfaces, Matrigel is frequently used to coat tissue culture plates, and ECs are plated in the presence of angiogenic or antiangiogenic molecules.[4,5] With appropriate angiogenic molecules, ECs organize into thin cords and eventually assemble into honeycomb-like structures within 4–8 h.[6] However, since Matrigel is composed of multiple ECM proteins and growth factors, it is difficult to delineate the specific interactions that stimulate angiogenesis. In more defined studies, individual ECM proteins were studied for their effects on angiogenesis. Capillary ECs were cultured on culture dishes precoated with varying concentrations of fibronectin, and cell spreading and growth were either stimulated or inhibited on highly adhesive ($>500\,ng/cm^2$) and nonadhesive ($<100\,ng/cm^2$) ECM substrate, respectively.[3,7] Interestingly, intermediate fibronectin coating densities ($100–500\,ng/cm^2$) promoted formation of EC tube networks within 1–2 days.

The density and geometry of ECM-coated substrate can be controlled more precisely with the various micropatterning techniques available. In particular, microcontact printing was utilized by several groups to study the effect of geometrical distribution of ECM proteins on morphogenesis of ECs into tubular structures.[8,9] In this technique,[10,11] poly(dimethyl siloxane) stamps were fabricated by casting the prepolymer against relief patterns, and the stamps were dipped into

Department of Bioengineering, Rice University, Houston, Texas.

solution with thiol-containing moieties. The stamps were then brought into conformal contact with a gold substrate, leaving the thiol moieties in patterns. In one study, microcontact printing of self-assembled monolayers of alkanethiolates was used to form islands of fibronectin with various geometries on gold, and ECs formed tubular structures on 10-μm-wide lines of fibronectin.[8,9,12] In another study, chitosan and gelatin were micropatterned via the microcontact printing method, and ECs similarly underwent capillary morphogenesis on 20-μm lines of gelatin.[12] These studies have demonstrated that the creation of a well-defined substrate by micropatterning can provide a useful tool for investigating the progress of angiogenesis. Although these studies employed micropatterning techniques to successfully isolate and study geometrical cues of the ECM, their systems were still confounded with various biochemical cues present in the ECM proteins, which participate in rather complex cellular interactions as these proteins present cells with multiple cell binding, growth factor binding, as well as cryptic domains.[13,14] Therefore, a more controlled system is required to isolate the geometrical cues from the biochemical cues of the ECM proteins.

Instead of using the mixture of ECM proteins or their individual components as discussed above, this current work utilized Arg-Gly-Asp-Ser (RGDS) incorporated into poly (ethylene glycol) diacrylate (PEGDA) hydrogels as the most basic substrate upon which blood vessel formation by ECs is studied. The hydrophilic and highly mobile backbone, PEG, resists nonspecific protein adsorption and cell adhesion.[15] On this nonadhesive surface, specific bioactive factors can be systemically added with precise control over both concentration and geometry to induce favorable cellular interactions. It has been previously reported that PEGDA hydrogels modified with various cell adhesive ligands support cell adhesion, proliferation, and migration of many different cell types.[15–18] Two-dimensional and three-dimensional (3D) micropatterning of these ligands in hydrogels also has been performed by photolithographic techniques to guide cell adhesion and migration.[19–22]

This work demonstrates a new application of synthetic, biomimetic PEGDA hydrogels as a biocompatible and bioactive substrate for induction and regulation of blood vessel formation. PEGDA hydrogels were micropatterned with RGDS in various densities and geometries via photolithographic technique, and EC morphogenesis into rudimentary capillary-like structures was induced and guided on these materials.

Materials and Methods

Cell maintenance

Human umbilical vein endothelial cells (HUVECs) were obtained from Cambrex (East Rutherford, NJ) and were grown on EC medium EGM-2 (Cambrex) supplemented with 2 mM L-glutamine, 1000 U/mL penicillin, and 100 mg/L streptomycin (Sigma, St. Louis, MO). Cells were incubated at 37°C in a 5% carbon dioxide environment. All experiments were conducted using cells from passages 3 to 8.

Synthesis of PEGDA

PEGDA was synthesized as described previously.[15] Briefly, 12 g dry PEG (6000 Da; Fluka, Milwaukee, WI) in 36 mL anhydrous dichloromethane was reacted with 0.25 g triethylamine and 0.43 g acryloyl chloride (Lancaster Synthesis, Windham, NH) under argon overnight. The resulting solution was washed with 2 M K_2CO_3 and separated into aqueous and organic phases. The organic phase was dried with anhydrous $MgSO_4$, and PEGDA was precipitated in diethyl ether, filtered, and dried under vacuum. The resulting product was analyzed by ^{1}H-NMR (Advance 400; Bruker, Hanau, Germany) with D_2O as a solvent.

Synthesis of PEG derivatives

The cell adhesive ligand, RGDS (American Peptide, Sunnyvale, CA), was conjugated to PEG monoacrylate by reaction with acrylate-PEG-*N*-hydroxysuccinimide (PEG-NHS, 3400 Da; Nektar, Huntsville, AL) in 1:1 molar ratio in 50 mM sodium bicarbonate buffer (pH 8.5) for 2 h at room temperature. The resultant product, PEG-RGDS, was dialyzed, lyophilized, and stored at −80°C. Horseradish peroxidase (HRP) (Sigma) was similarly reacted with PEG-NHS and subsequently with fluorescein-5-isothiocyanate (FITC) (Invitrogen, Carlsbad, CA) in 1:10 molar ratio for 1 h at room temperature. The resultant product, PEG-HRP-FITC, was used to aid in visualization of the surface-patterned areas on the hydrogels. A gel permeation chromatography system equipped with ultraviolet (UV)-vis and evaporative light scattering detectors (GPC; Polymer Laboratories, Amherst, MA) was used to confirm PEG conjugation to RGDS.

Surface patterning of PEGDA hydrogels

Single or multiple bioactive molecules have been immobilized on the surface of PEGDA hydrogels with great fidelity using photolithographic techniques, and the amount bound has been shown to be precisely controlled by their initial concentration in the prepolymer solution or the duration of exposure of the UV lamp during photopolymerization.[20] Surface patterning on PEGDA hydrogels involved two successive photopolymerization steps. First, base cell-nonadhesive PEGDA hydrogels were prepared by pouring 0.1 g/mL PEGDA in 10 mM HEPES-buffered saline (pH 7.4) into rectangular glass molds (0.5-mm thickness), and exposing the polymer solution to long-wavelength UV light (365 nm, 10 mW/cm^2) for 30 s. After rinsing the hydrogels with phosphate-buffered saline (PBS; pH 7.4), the surfaces of the hydrogels were covered evenly with 50 μL of a second polymer solution containing various concentrations of PEG-RGDS in 10 mM HEPES-buffered saline (pH 7.4).

The thin layer of prepolymer solution was covered using transparency masks with desired patterns, which were prepared using Illustrator and a standard laser jet printer (LaserWriter 16/600 PS; Apple Computers, Cupertino, CA). Subsequent second exposure to UV light for 1 min allowed conjugation of acrylated PEG-RGDS to unreacted acrylates on the hydrogels, forming a covalently bound layer of PEG-RGDS in patterns on the surface of the base PEGDA hydrogels. The surface PEG-RGDS concentrations reported in this study were calculated from the amount of PEG-RGDS applied on the surface of PEGDA hydrogels.

To visualize the patterned areas on the hydrogels, PEG-HRP-FITC was used instead of PEG-RGDS and examined with an epi-fluorescence microscope (Axiovert 135; Carl Zeiss,

Thornwood, NY). All polymer solutions contained 10 μL/mL of 2,2-dimethyl-2-phenyl-acetophenone in *N*-vinylpyrrolidone (300 mg/mL) as a photoinitiator. Unbound peptides were rinsed from the hydrogels during 2-h incubation in EGM-2 media. Finally, the hydrogels were cut into discs with 2.0-cm diameter and placed in 24-well plates.

HUVEC adhesion on PEGDA hydrogels

Cell adhesion was evaluated on the surface of PEGDA hydrogels patterned with various concentrations of PEG-RGDS. Hydrogel samples were prepared with PEG-RGDS concentrations of 2, 4, 20, and 100 $\mu g/cm^2$ patterned into 50-μm-wide stripes. HUVECs (45,000 cells/cm^2) were plated, and after 1 day in culture, nonadherent cells were removed with a PBS wash. Cells were photographed with a digital camera (Nikon, Melville, NY) mounted on a phase contrast microscope (Axiovert 135; Carl Zeiss). The adherent cells on each hydrogel were trypsinized, and the cell number was measured using a Coulter counter (Coulter, Fullerton, CA).

Tube formation and visualization

To examine the effect of patterned RGDS concentration on EC cord formation, HUVECs (45,000 cells/cm^2) were seeded on PEGDA hydrogel surface patterned with 50-μm-wide stripes of PEG-RGDS at various concentrations, ranging from 2 to 100 $\mu g/cm^2$. HUVECs cultured for 2 days on the patterned stripes were fixed in 3.7% formaldehyde in PBS for 15 min, followed by permeabilization with 0.5% Triton X-100 in PBS for 10 min. The specimens were blocked with 3% bovine serum albumin (BSA; Sigma) in PBS for 30 min, and actin and nuclei were stained with tetramethyl rhodamine isothiocyanate (TRITC)-conjugated phalloidin (5 U/mL; Sigma) for 1 h and 4′,6-diamidino-2-phenylindole (DAPI) (300 nM; Invitrogen) for 5 min. Confocal imaging was performed on a Zeiss LSM 510 META system (Carl Zeiss).

To investigate the effect of patterned geometry on EC cord formation, HUVECs (45,000 cells/cm^2) were seeded on PEG-DA hydrogels with surface-patterned PEG-RGDS (20 $\mu g/cm^2$) on stripes with width ranging from 50 to 200 μm. On days 1 and 18 after cell seeding, random areas in each sample were photographed to visualize changes in cell morphology before and after EC cord formation. Expression patterns of ECM proteins were also visualized with immunofluorescence staining. The specimens were fixed, permeabilized, and blocked as described previously, and they were incubated with primary antibodies against fibronectin, laminin, or collagen type I (diluted to 1:25 with 3% BSA in PBS; Sigma) for 2 h and with a secondary antibody conjugated to Alexa fluor 488 (diluted to 1:1000 in 3% BSA in PBS; Invitrogen) for 1 h. The specimens were visualized with an epi-fluorescence microscope (Axiovert 135; Carl Zeiss).

Statistical analysis

Statistical analysis was performed with Jmp 5.1 (SAS Institute, Cary, NC). Data sets were analyzed using one-way analysis of variance (ANOVA), followed by Tukey's honestly significant difference (HSD) test for multiple comparisons. *p*-values less than 0.05 were considered statistically significant. All values are reported as mean ± standard deviation.

Results

Surface patterning of PEGDA hydrogels

A surface patterning technique to immobilize peptides on PEGDA hydrogels using photolithography was recently developed, and various geometries have been patterned onto hydrogel surfaces.[20] In this current work, straight lines with varying widths were patterned with bioactive molecules in order to promote EC cord formation on PEGDA hydrogels. Clear transparencies were laser printed with stripes leaving 50- and 200-μm-wide blank lines (Fig. 1A). To aid in visualization, PEG conjugated to FITC was applied on the surface of hydrogel, and the acrylate moieties were immobilized selectively on specific regions by applying UV light through the transparency for 1 min. After 2 h of washing, FITC-bound stripes with width corresponding to the original patterns were observed, confirming the successful surface patterning on the hydrogels (Fig. 1B).

In order to demonstrate feasibility of guiding HUVEC adhesion on hydrogels with micropatterned RGDS, the hydrogels were surface patterned with high enough concentration of PEG-RGDS to allow cell adhesion. PEG-RGDS of 300 $\mu g/cm^2$ was applied on the cell-nonadhesive PEGDA hydrogels and exposed to a UV source through the transparency masks. The resulting PEGDA hydrogels were seeded with HUVECs, and after 1 day in culture, the cells were found to adhere and spread only on 50- and 200-μm-wide stripes immobilized with PEG-RGDS, but not on bare PEGDA regions (Fig. 1C).

HUVEC adhesion on various concentrations of RGDS

In order to optimize the hydrogel culture system for HUVEC adhesion and cord formation, various concentrations of PEG-RGDS were patterned onto 50-μm-wide stripes, and HUVEC adhesion was assessed after 1 day of seeding (Fig. 2). On 50-μm-wide stripes patterned with 2.0 $\mu g/cm^2$ of PEG-RGDS, there was minimal cell adhesion as the cells failed to attach or spread on the hydrogels. When PEG-RGDS concentration was increased to 4.0 $\mu g/cm^2$, some areas along the stripes were covered by HUVECs. With 20 and 100 $\mu g/cm^2$ of PEG-RGDS, HUVECs attached and covered all regions of 50-μm-wide stripes. The progressive increase in HUVEC adhesion was quantified by counting the number of attached cells on hydrogels. As PEG-RGDS concentration was increased from 2.0 to 100 $\mu g/cm^2$, HUVEC adhesion correspondingly increased as shown in Figure 2B.

Modulation of endothelial morphogenesis by the PEG-RGDS concentration

In order to examine the effect of RGDS concentration on EC cord formation, HUVECs were cultured on 50-μm-wide stripes patterned with various concentrations of PEG-RGDS, ranging from 2.0 to 100 $\mu g/cm^2$. At low concentration of PEG-RGDS at 2.0 or 4.0 $\mu g/cm^2$, there was minimal number of HUVECs remaining attached to the substrates after 2 days in culture as described above. On the other hand, HUVECs cultured on stripes with intermediate PEG-RGDS concentration of 20 $\mu g/cm^2$ underwent morphogenesis and condensed into highly organized, cord-like structures along the length of the stripes (Fig. 3A). A vertical cross section of one such region shows that HUVECs in the center began to protrude their

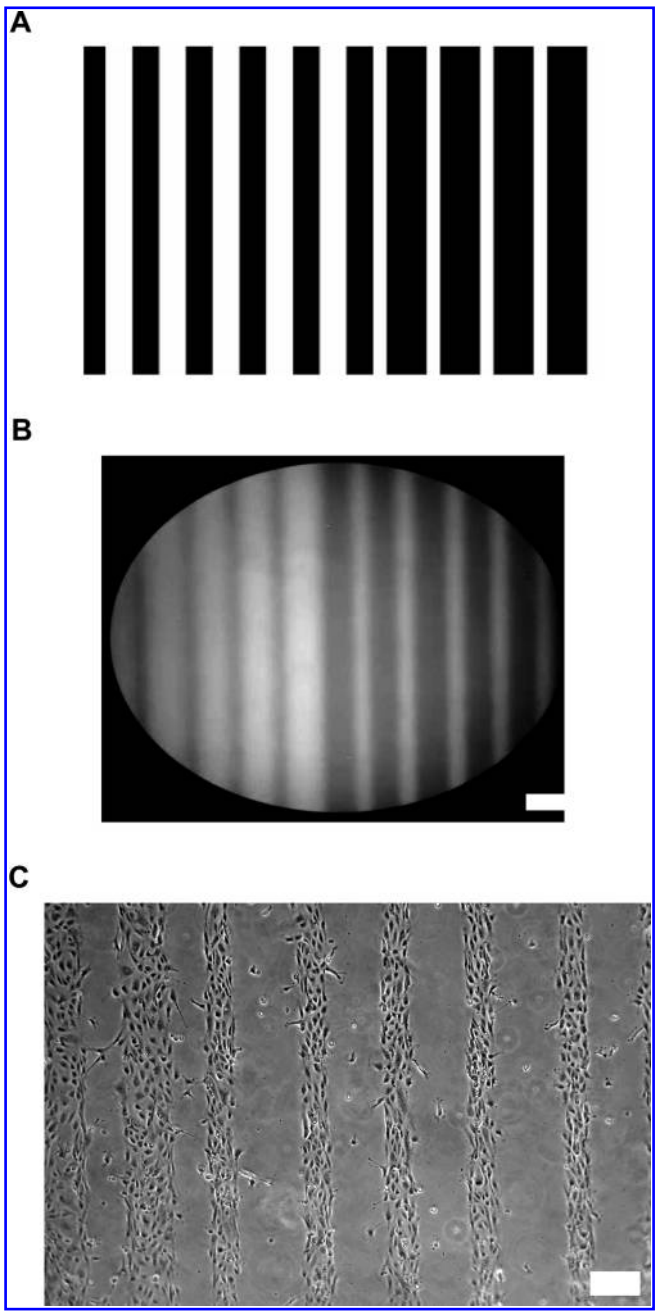

FIG. 1. Surface patterning of PEGDA hydrogels. (**A**) Stripes with 50- and 200-μm widths were laser printed on transparency mask. (**B**) Fluorescence image of PEGDA hydrogel surface patterned with FITC-conjugated PEG confirming successful patterning. (**C**) HUVEC adhesion on a hydrogel patterned with PEG-RGDS. Scale bars = 200 μm.

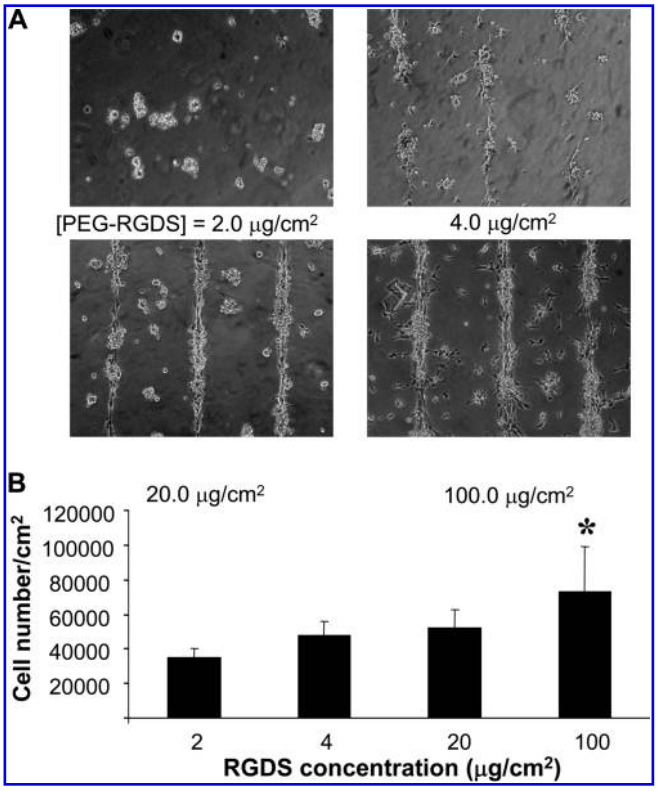

FIG. 2. The effects of PEG-RGDS concentration in micropatterns on HUVEC adhesion. (**A**) HUVECs attached on the surface of PEGDA hydrogels patterned with various concentrations of PEG-RGDS in 50-μm-wide stripes. (**B**) Quantification of cell adhesion by Coulter counter showed increasing number of attached cells with increasing concentration of PEG-RGDS on PEGDA hydrogels. Data represent mean ± SD ($n = 5$). *$p < 0.05$, analyzed by one-way ANOVA followed by Tukey's HSD test.

nuclei and cell bodies vertically upward, and multiple cells were stacked on top of each other (Fig. 3A). This phenomenon resulted in the formation of 3D cord-like structures assembled solely by HUVECs on 2D surface of PEGDA hydrogels. In contrast, HUVECs cultured on stripes with higher PEG-RGDS concentrations failed to undergo morphogenesis. On stripes with 40 or 100 μg/cm^2 of PEG-RGDS, HUVECs retained their typical cobble stone–like morphology, and a vertical cross section of one such region shows that the cells remained well spread as monolayer close to the substrates (only 100 μg/cm^2 shown in Fig. 3B).

Modulation of endothelial morphogenesis by the width of patterned stripes

In order to guide EC cord formation on the PEGDA hydrogels, the width of PEG-RGDS patterns were varied, and their effects on cord formation were examined (Fig. 4). HUVECs were seeded on stripes with width ranging from 50 to 200 μm. These stripes were prepared with 20 μg/cm^2 of PEG-RGDS, which is the concentration found to support EC morphogenesis as described above. After cell seeding, HUVEC morphology was monitored up to 18 days. On 50-μm-wide stripes, HUVECs formed highly organized contiguous cord-like structures in parallel orientation by 18 days in culture (Fig. 4). On the other hand, most cells cultured on 75-, 100-, or 200-μm-wide stripes remained well spread up to 18 days in culture (only 200-μm-wide stripes shown in Fig. 4).

ECM protein expression during HUVEC morphogenesis

Expression of ECM proteins during morphogenesis was also investigated using immunofluorescence staining. After

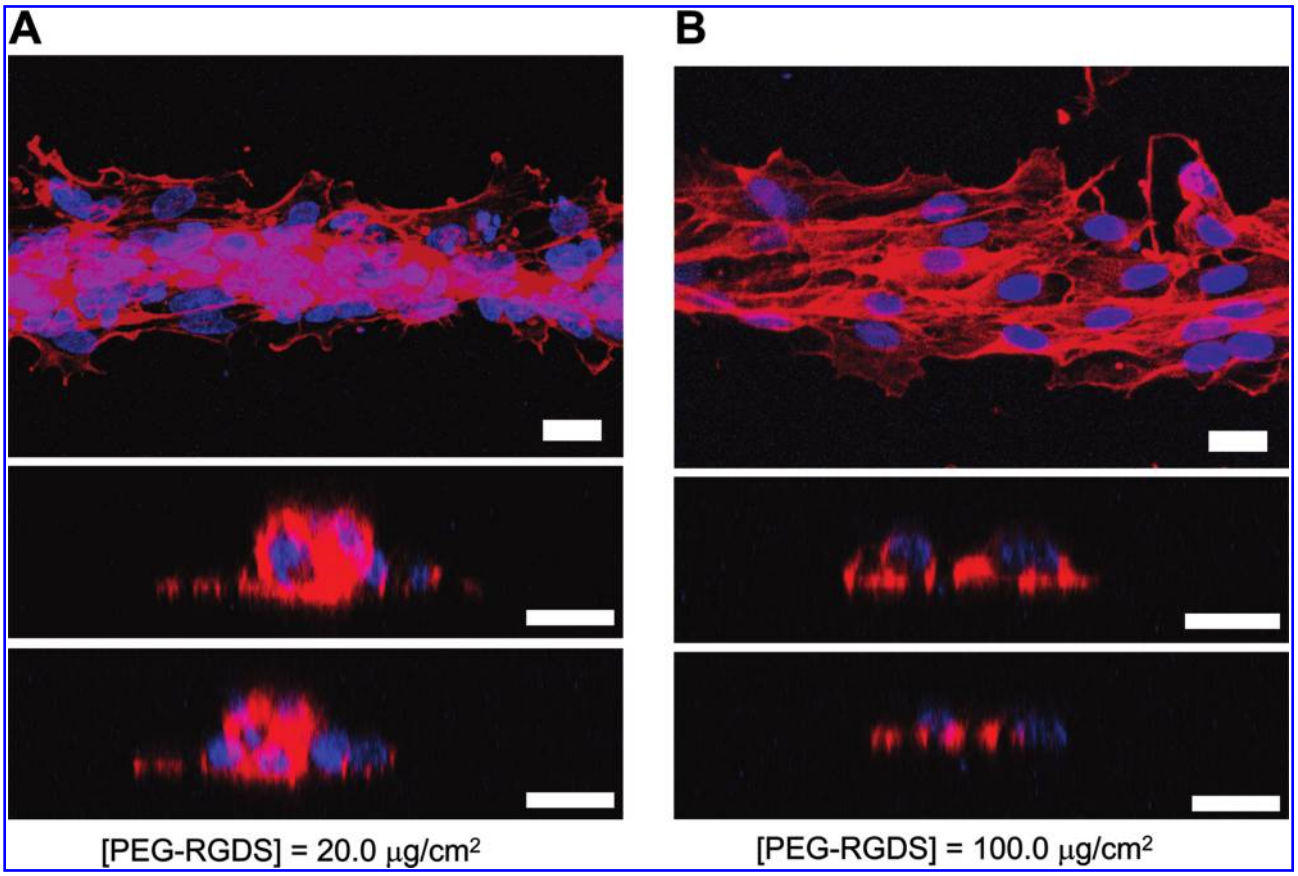

FIG. 3. Visualization of EC morphogenesis on PEGDA hydrogels. (**A**) Confocal images showing HUVECs undergoing cord formation on 50-μm-wide stripes with PEG-RGDS at 20 μg/cm^2 after 2 days in culture. HUVECs coalesced into dense, cord-like structures along the central axis of the stripe. (**B**) In contrast, HUVECs cultured on stripes with PEG-RGDS at 100 μg/cm^2 remained on monolayer. Cells stained with TRITC-phalloidin and DAPI are shown in red and blue, respectively. Scale bars = 20 μm.

14 days in culture, HUVECs in the process of cord formation on RGDS stripes with 50-μm width were found to produce a significant amount of fibronectin and laminin along the length of cords, whereas deposition of collagen type I was below the detection level (Fig. 5). The samples incubated with anti-rabbit and anti-mouse secondary antibodies conjugated with Alexa fluor 488 had minimal background fluorescence.

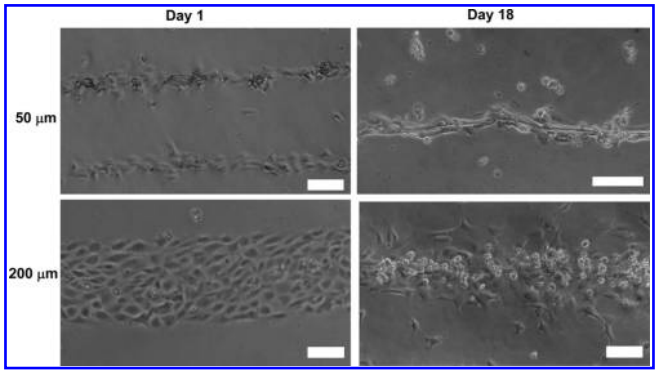

FIG. 4. Cord formation by HUVECs seeded on PEGDA hydrogels micropatterned with PEG-RGDS. EC morphogenesis is differentially regulated by the width of RGDS stripes on PEGDA hydrogels. HUVECs formed cord-like structures on 50-μm-wide stripes patterned with 20 μg/cm^2 of PEG-RGDS, but not on 200-μm-wide stripes. Scale bars = 100 μm.

Discussion

In this study, a surface patterning technique was developed to regulate the process of EC morphogenesis on synthetic PEGDA hydrogels. Specifically, a photolithographic method was employed to vary the density and geometry of PEG-RGDS displayed on PEGDA hydrogels in order to modulate EC angiogenesis. ECs cultured on RGDS stripes underwent morphogenesis and formed rudimentary capillary-like structures depending on the width and density of the RGDS patterns.

ECs grown on wide stripes remained in a normal, static state, while restricting the geometries of the patterned area to 50 μm seems to send angiogenic cues to ECs and stimulates reorganization of the cell bodies into cord structures. Concentration of RGDS also modulated EC morphogenesis; endothelial cord formation was stimulated on intermediate concentration of RGDS (20 μg/cm^2) sufficient to sustain cell adhesion, whereas it was inhibited on higher concentration of RGDS that supported firm cell adhesion. The cords formed by ECs were reminiscent of capillaries with cells participating in the self-assembly and reorganization into multicellular

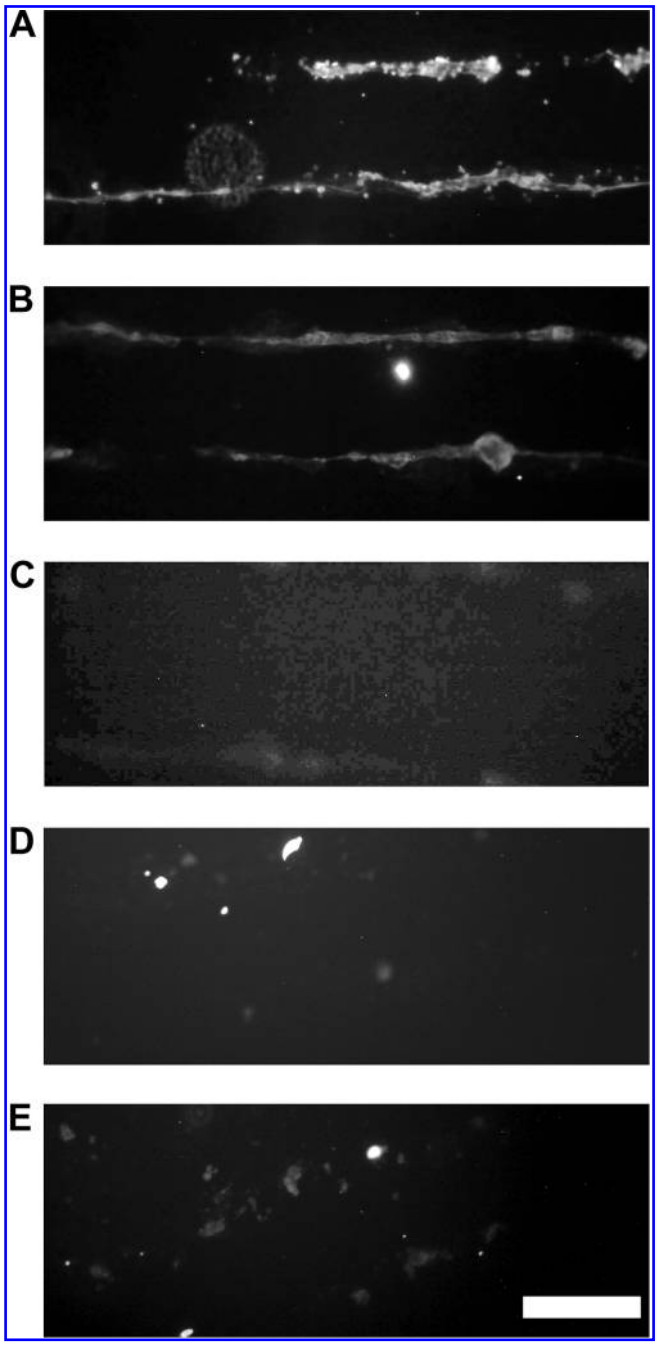

FIG. 5. Expression of ECM proteins during EC morphogenesis. After 14 days in culture, HUVECs produced (**A**) fibronectin, (**B**) laminin, but not detectable amount of (**C**) collagen type I on 50-μm-wide stripes of PEG-RGDS. Secondary antibody controls with (**D**) anti-rabbit IgG and (**E**) anti-mouse IgG had minimal background signal. Scale bar = 200 μm.

structures. This work has demonstrated that a well-defined substrate created by micropatterning can provide useful tools to regulate capillary morphogenesis and to investigate the progress of angiogenesis.

Only a handful of studies have reported regulation of EC morphogenesis by micropatterned ECM substrates. Dike *et al.* created stripes of fibronectin using microcontact printing on gold surface.[9] ECs cultured for 3 days on 10-μm-wide stripes escaped the growth phase and underwent capillary morphogenesis. However, ECs cultured on 30-μm-wide lines continued to proliferate and maintained their normal morphologies. In a more recent work, human microvascular ECs cultured on 20-μm lines of micropatterned gelatin substrates formed tubule-like structures.[12] It was noteworthy in these studies that the width of fibronectin or gelatin stripes required for ECs to initiate tubulogenesis was 10–20 μm, whereas EC morphogenesis was inhibited on wider stripes. In contrast, in this current system employing RGDS, we observed endothelial tube formation on PEG-RGDS stripes as wide as 50 μm, but not on wider stripes. Multiple cell binding domains as well as any growth factors bound on ECM proteins seem to potentiate the angiogenic cues derived from the restriction of ECM geometry in a synergistic manner, and this may explain the different results obtained in this current study compared to the aforementioned studies.

There have been several studies that examined the effect of ligand concentration on angiogenesis. It is generally hypothesized that the angiogenic cue is derived from changes in cell shape that is regulated by the density of immobilized cell adhesion ligand. EC morphogenesis is known to be promoted on intermediate fibronectin coating densities (100–500 ng/cm^2), whereas highly adhesive (>500 ng/cm^2) and nonadhesive (<100 ng/cm^2) coating densities promote cell growth and apoptosis, respectively.[7,23] It has been further shown that the switch between growth or apoptosis of a single EC is regulated by the degree to which the cell spreads on micropatterned surfaces.[24] Deriving from these previous studies, the current study aimed to find the optimal concentration of cell adhesion ligand, RGDS, at which EC morphogenesis can be promoted and guided in predesigned geometries. EC cord formation was promoted at intermediate concentration of RGDS as well as on narrow RGDS stripes; identification of these two conditions will allow fabrication of scaffold materials with patterned endothelial blood vessel structures in large scale.

ECM proteins are critical during angiogenesis. Collagen I fibers have been suggested to provide a scaffold upon which ECs align and form capillary structures,[25] and its expression in the capillaries appears to be coincident with angiogenesis as ECs that do not express collagen I fail to form cords or tubes in culture.[26] In this regard, it is notable that ECs produced fibronectin and laminin but not collagen I on micropatterns. The discrepancy on expression of collagen type I during EC morphogenesis warrants further studies as it is plausible that fibronectin and laminin but not collagen I play essential roles in the early phase of blood vessel formation.[27]

Work presented here examined the efficacy of PEGDA hydrogels as a scaffold material to promote neovascularization. The fact that ECs underwent cord formation on PEGDA hydrogels demonstrates that PEGDA hydrogel is a suitable biomaterial to orchestrate and recapitulate intricate process of neovascularization. Absence of complex cellular interactions with ECM proteins as well as precise control over the constituents of the scaffold material makes PEGDA hydrogels a versatile test bed for vascular biology and pharmacological studies. In addition, identification of the hydrogels as an amenable environment for blood vessel formation demon-

strates that this material holds great potentials for various applications in tissue engineering, where prevascularization of tissue implants is critical.

In order to build scaffold materials that can be used in clinical settings, the current study has to be extended to biodegradable PEG hydrogels that allow mammalian enzymes to degrade the matrices for facile integration with host tissue.[16,17] Also, the current system can be used to build scalable, 3D structures by stacking multiple layers of hydrogels with patterned blood vessels.[20] The organization of cells in predesigned shapes and promotion of their morphogenesis into blood vessel–like structures are an important first step toward the fabrication of engineered tissues with complex architecture.

Acknowledgments

This work was supported by NIH and NSF. The authors would like to thank Melissa McHale for critical review of the manuscript.

References

1. Davis, G.E., Bayless, K.J., and Mavila, A. Molecular basis of endothelial cell morphogenesis in three-dimensional extracellular matrices. Anat Rec **268,** 252, 2002.
2. Jain, R.K. Molecular regulation of vessel maturation. Nat Med **9,** 685, 2003.
3. Folkman, J., and Haudenschild, C. Angiogenesis *in vitro*. Nature **288,** 551, 1980.
4. Egginton, S., and Gerritsen, M. Lumen formation: *in vivo* versus *in vitro* observations. Microcirculation **10,** 45, 2003.
5. Ponce, M.L. *In vitro* matrigel angiogenesis assays. In: Murray, J.C., ed. Angiogenesis Protocols. Totowa, NJ: Humana Press, 2001, p. 205.
6. Kubota, Y., Kleinman, H.K., Martin, G.R., and Lawley, T.J. Role of laminin and basement membrane in the morphological differentiation of human endothelial cells into capillary-like structures. J Cell Biol **107,** 1589, 1988.
7. Ingber, D.E., and Folkman, J. Mechanochemical switching between growth and differentiation during fibroblast growth factor-stimulated angiogenesis *in vitro*: role of extracellular matrix. J Cell Biol **109,** 317, 1989.
8. Chen, C.S., Mrksich, M., Huang, S., Whitesides, G.M., and Ingber, D.E. Micropatterned surfaces for control of cell shape, position, and function. Biotechnol Prog **14,** 356, 1998.
9. Dike, L.E., Chen, C.S., Mrksich, M., Tien, J., Whitesides, G.M., and Ingber, D.E. Geometric control of switching between growth, apoptosis, and differentiation during angiogenesis using micropatterned substrates. *In Vitro* Cell Dev Biol Anim **35,** 441, 1999.
10. Mrksich, M., Chen, C.S., Xia, Y., Dike, L.E., Ingber, D.E., and Whitesides, G.M. Controlling cell attachment on contoured surfaces with self-assembled monolayers of alkanethiolates on gold. Proc Natl Acad Sci USA **93,** 10775, 1996.
11. Prime, K., and Whitesides, G. Self-assembled organic monolayers: model systems for studying adsorption of proteins at surfaces. Science **252,** 1164, 1991.
12. Co, C.C., Wang, Y.C., and Ho, C.C. Biocompatible micropatterning of two different cell types. J Am Chem Soc **127,** 1598, 2005.
13. Romberger, D.J. Fibronectin. Int J Biochem Cell Biol **29,** 939, 1997.
14. Wierzbicka-Patynowski, I., and Schwarzbauer, J.E. The ins and outs of fibronectin matrix assembly. J Cell Sci **116,** 3269, 2003.
15. DeLong, S.A., Moon, J.J., and West, J.L. Covalently immobilized gradients of bFGF on hydrogel scaffolds for directed cell migration. Biomaterials **26,** 3227, 2005.
16. Mann, B.K., Gobin, A.S., Tsai, A.T., Schmedlen, R.H., and West, J.L. Smooth muscle cell growth in photopolymerized hydrogels with cell adhesive and proteolytically degradable domains: synthetic ECM analogs for tissue engineering. Biomaterials **22,** 3045, 2001.
17. Lee, S.H., Miller, J.S., Moon, J.J., and West, J.L. Proteolytically degradable hydrogels with a fluorogenic substrate for studies of cellular proteolytic activity and migration. Biotechnol Prog **21,** 1736, 2005.
18. Patel, P.N., Gobin, A.S., West, J.L., and Patrick, C.W. Poly(ethylene glycol) hydrogel system supports preadipocyte viability, adhesion, and proliferation. Tissue Eng **11,** 1498, 2005.
19. Hahn, M.S., Miller, J.S., and West, J.L. Laser scanning lithography for surface micropatterning on hydrogels. Adv Mater **17,** 2939, 2005.
20. Hahn, M.S., Taite, L.J., Moon, J.J., Rowland, M.C., Ruffino, K.A., and West, J.L. Photolithographic patterning of polyethylene glycol hydrogels. Biomaterials **27,** 2519, 2006.
21. Hahn, M.S., Miller, J.S., and West, J.L. Three-dimensional biochemical and biomechanical patterning of hydrogels for guiding cell behavior. Adv Mater **18,** 2679, 2006.
22. Lee, S.H., Moon, J.J., and West, J.L. Three-dimensional micropatterning of bioactive hydrogels via two-photon laser scanning photolithography for guided 3D cell migration. Biomaterials **29,** 2962, 2008.
23. Ingber, D.E. Fibronectin controls capillary endothelial cell growth by modulating cell shape. Proc Natl Acad Sci USA **87,** 3579, 1990.
24. Chen, C.S., Mrksich, M., Huang, S., Whitesides, G.M., and Ingber, D.E. Geometric control of cell life and death. Science **276,** 1425, 1997.
25. Vernon, R.B., and Sage, E.H. Between molecules and morphology—extracellular-matrix and creation of vascular form. Am J Pathol **147,** 873, 1995.
26. Vernon, R.B., Lara, S.L., Drake, C.J., Iruelaarispe, M.L., Angello, J.C., Little, C.D., Wight, T.N., and Sage, E.H. Organized type-I collagen influences endothelial patterns during spontaneous angiogenesis *in vitro*—planar cultures as models of vascular development. *In Vitro* Cell Dev Biol Anim **31,** 120, 1995.
27. Lohler, J., Timpl, R., and Jaenisch, R. Embryonic lethal mutation in mouse collagen-I gene causes rupture of blood-vessels and is associated with erythropoietic and mesenchymal cell-death. Cell **38,** 597, 1984.

Address reprint requests to:
Jennifer L. West, Ph.D.
Department of Bioengineering
Rice University
P.O. Box 1892, MS 142
Houston, TX 77251–1892

E-mail: jwest@rice.edu

Received: April 1, 2008
Accepted: June 2, 2008
Online Publication Date: September 15, 2008

This article has been cited by:

1. Geraldine Koenig, Hayriye Ozcelik, Lisa Haesler, Martina Cihova, Sait Ciftci, Agnes Dupret-Bories, Christian Debry, Martin Stelzle, Philippe Lavalle, Nihal Engin Vrana. 2016. Cell-laden hydrogel/titanium microhybrids: Site-specific cell delivery to metallic implants for improved integration. *Acta Biomaterialia* **33**, 301-310. [CrossRef]
2. Xuetao Sun, Wafa Altalhi, Sara S. Nunes. 2016. Vascularization strategies of engineered tissues and their application in cardiac regeneration. *Advanced Drug Delivery Reviews* **96**, 183-194. [CrossRef]
3. Qihui Zhou, Philipp T. Kühn, Thirsa Huisman, Elsje Nieboer, Charlotte van Zwol, Theo G. van Kooten, Patrick van Rijn. 2015. Directional nanotopographic gradients: a high-throughput screening platform for cell contact guidance. *Scientific Reports* **5**, 16240. [CrossRef]
4. Samad Ahadian, Ramin Banan Sadeghian, Sahar Salehi, Serge Ostrovidov, Hojae Bae, Murugan Ramalingam, Ali Khademhosseini. 2015. Bioconjugated Hydrogels for Tissue Engineering and Regenerative Medicine. *Bioconjugate Chemistry* **26**, 1984-2001. [CrossRef]
5. Sadik Kaga, Serap Yapar, Ece Manavoglu Gecici, Rana Sanyal. 2015. Photopatternable "Clickable" Hydrogels: "Orthogonal" Control over Fabrication and Functionalization. *Macromolecules* **48**, 5106-5115. [CrossRef]
6. Jingjing Zhang, Ayeesha Mujeeb, Yanan Du, Jianhao Lin, Zigang Ge. 2015. Probing cell–matrix interactions in RGD-decorated macroporous poly (ethylene glycol) hydrogels for 3D chondrocyte culture. *Biomedical Materials* **10**, 035016. [CrossRef]
7. M. Ogawa, K. Higashi, N. MikiMicrobial production inside microfabricated hydrogel microtubes 1692-1694. [CrossRef]
8. Michael R Blatchley, Sharon Gerecht. 2015. Acellular implantable and injectable hydrogels for vascular regeneration. *Biomedical Materials* **10**, 034001. [CrossRef]
9. Julia E. Samorezov, Eben Alsberg. 2015. Spatial regulation of controlled bioactive factor delivery for bone tissue engineering. *Advanced Drug Delivery Reviews* **84**, 45-67. [CrossRef]
10. Vincenzo Guarino, Michele Galizia, Marco Alvarez-Perez, Giuseppe Mensitieri, Luigi Ambrosio. 2015. Improving surface and transport properties of macroporous hydrogels for bone regeneration. *Journal of Biomedical Materials Research Part A* **103**, 1095-1105. [CrossRef]
11. David C. Sullivan, Jonathan P. Repper, Adam W. Frock, Peter S. McFetridge, Bryon E. Petersen. 2015. Current Translational Challenges for Tissue Engineering: 3D Culture, Nanotechnology, and Decellularized Matrices. *Current Pathobiology Reports* **3**, 99-106. [CrossRef]
12. Michael Blatchley, Kyung Min Park, Sharon Gerecht. 2015. Designer hydrogels for precision control of oxygen tension and mechanical properties. *J. Mater. Chem. B* **3**, 7939-7949. [CrossRef]
13. Mohammad Izadifar, Michael E. Kelly, Xiongbiao Chen. 2014. Engineering Angiogenesis for Myocardial Infarction Repair: Recent Developments, Challenges, and Future Directions. *Cardiovascular Engineering and Technology* **5**, 281-307. [CrossRef]
14. Kyung Min Park, Sharon GerechtBiomaterials as Artificial Niches for Pluripotent Stem Cell Engineering 21-43. [CrossRef]
15. Li Cheri Y., Stevens Kelly R., Schwartz Robert E., Alejandro Brian S., Huang Joanne H., Bhatia Sangeeta N.. 2014. Micropatterned Cell–Cell Interactions Enable Functional Encapsulation of Primary Hepatocytes in Hydrogel Microtissues. *Tissue Engineering Part A* **20**:15-16, 2200-2212. [Abstract] [Full Text HTML] [Full Text PDF] [Full Text PDF with Links] [Supplemental Material]
16. Anwarul Hasan, Arghya Paul, Nihal E. Vrana, Xin Zhao, Adnan Memic, Yu-Shik Hwang, Mehmet R. Dokmeci, Ali Khademhosseini. 2014. Microfluidic techniques for development of 3D vascularized tissue. *Biomaterials* **35**, 7308-7325. [CrossRef]
17. Aleixandre Rodrigo-Navarro, Patricia Rico, Anas Saadeddin, Andres J. Garcia, Manuel Salmeron-Sanchez. 2014. Living biointerfaces based on non-pathogenic bacteria to direct cell differentiation. *Scientific Reports* **4**. . [CrossRef]
18. Rui Yao, Jingyu Wang, Xiaokang Li, Jung Da, Hao Qi, Keh Kooi Kee, Yanan Du. 2014. Hepatic Differentiation of Human Embryonic Stem Cells as Microscaled Multilayered Colonies Leading to Enhanced Homogeneity and Maturation. *Small* n/a-n/a. [CrossRef]
19. Vivian Lee, Guohao DaiMicro and Nanotechnology in Vascular Regeneration 695-724. [CrossRef]
20. Joseph Hoffmann, Jennifer WestThree-Dimensional Micropatterning of Biomaterial Scaffolds for Tissue Engineering 37-74. [CrossRef]
21. M. Deforet, V. Hakim, H.G. Yevick, G. Duclos, P. Silberzan. 2014. Emergence of collective modes and tri-dimensional structures from epithelial confinement. *Nature Communications* **5**. . [CrossRef]
22. Sonja Sokic, Megan Christenson, Jeffery Larson, Georgia Papavasiliou. 2014. In Situ Generation of Cell-Laden Porous MMP-Sensitive PEGDA Hydrogels by Gelatin Leaching. *Macromolecular Bioscience* **14**, 731-739. [CrossRef]

23. Marine Verhulsel, Maéva Vignes, Stéphanie Descroix, Laurent Malaquin, Danijela M. Vignjevic, Jean-Louis Viovy. 2014. A review of microfabrication and hydrogel engineering for micro-organs on chips. *Biomaterials* **35**, 1816-1832. [CrossRef]
24. Julien Barthes, Hayriye Özçelik, Mathilde Hindié, Albana Ndreu-Halili, Anwarul Hasan, Nihal Engin Vrana. 2014. Cell Microenvironment Engineering and Monitoring for Tissue Engineering and Regenerative Medicine: The Recent Advances. *BioMed Research International* **2014**, 1-18. [CrossRef]
25. Saniya Ali, Maude L. Cuchiara, Jennifer L. WestMicropatterning of Poly(ethylene glycol) Diacrylate Hydrogels 105-119. [CrossRef]
26. S. Kusuma, L.E. Dickinson, S. GerechtCell–biomaterial interactions for blood vessel formation 350-388. [CrossRef]
27. Claudio Muscari, Emanuele Giordano, Francesca Bonafè, Marco Govoni, Carlo Guarnieri. 2014. Strategies Affording Prevascularized Cell-Based Constructs for Myocardial Tissue Engineering. *Stem Cells International* **2014**, 1-8. [CrossRef]
28. Abdul Jalil Rufaihah, Srirangam Ramanujam Vaibavi, Marian Plotkin, Jiayi Shen, Venkateswaran Nithya, Jing Wang, Dror Seliktar, Theodoros Kofidis. 2013. Enhanced infarct stabilization and neovascularization mediated by VEGF-loaded PEGylated fibrinogen hydrogel in a rodent myocardial infarction model. *Biomaterials* **34**, 8195-8202. [CrossRef]
29. Anas Saadeddin, Aleixandre Rodrigo-Navarro, Vicente Monedero, Patricia Rico, David Moratal, María Luisa González-Martín, David Navarro, Andrés J. García, Manuel Salmerón-Sánchez. 2013. Functional Living Biointerphases. *Advanced Healthcare Materials* **2**:10.1002/adhm.v2.9, 1213-1218. [CrossRef]
30. François A. Auger, Laure Gibot, Dan Lacroix. 2013. The Pivotal Role of Vascularization in Tissue Engineering. *Annual Review of Biomedical Engineering* **15**, 177-200. [CrossRef]
31. Phat L. Tran, Jessica R. Gamboa, Katherine E. McCracken, Mark R. Riley, Marvin J. Slepian, Jeong-Yeol Yoon. 2013. Nanowell-Trapped Charged Ligand-Bearing Nanoparticle Surfaces: A Novel Method of Enhancing Flow-Resistant Cell Adhesion. *Advanced Healthcare Materials* **2**:10.1002/adhm.v2.7, 1019-1027. [CrossRef]
32. Boudewijn van der Sanden, Florence Appaix, François Berger, Laurent Selek, Jean-Paul Issartel, Didier Wion. 2013. Translation of the ecological trap concept to glioma therapy: the cancer cell trap concept. *Future Oncology* **9**, 817-824. [CrossRef]
33. Vincent E.G. Diederich, Peter Studer, Anita Kern, Marco Lattuada, Giuseppe Storti, Ram I. Sharma, Jess G. Snedeker, Massimo Morbidelli. 2013. Bioactive polyacrylamide hydrogels with gradients in mechanical stiffness. *Biotechnology and Bioengineering* **110**:10.1002/bit.v110.5, 1508-1519. [CrossRef]
34. Yifeng Lei, Omar F. Zouani, Lila Rami, Christel Chanseau, Marie-Christine Durrieu. 2013. Modulation of Lumen Formation by Microgeometrical Bioactive Cues and Migration Mode of Actin Machinery. *Small* **9**:10.1002/smll.v9.7, 1086-1095. [CrossRef]
35. Michael V Turturro, Sonja Sokic, Jeffery C Larson, Georgia Papavasiliou. 2013. Effective tuning of ligand incorporation and mechanical properties in visible light photopolymerized poly(ethylene glycol) diacrylate hydrogels dictates cell adhesion and proliferation. *Biomedical Materials* **8**, 025001. [CrossRef]
36. Catherine A. Goubko, Ajoy Basak, Swapan Majumdar, Harold Jarrell, Nam Huan Khieu, Xudong Cao. 2013. Comparative analysis of photocaged RGDS peptides for cell patterning. *Journal of Biomedical Materials Research Part A* **101A**:10.1002/jbm.a.v101a.3, 787-796. [CrossRef]
37. Li-Yang Jiang, Ying Luo. 2013. Guided assembly of endothelial cells on hydrogel matrices patterned with microgrooves: a basic model for microvessel engineering. *Soft Matter* **9**, 1113-1121. [CrossRef]
38. Melissa K. McHale, Nicole M. Bergmann, Jennifer L. WestHistogenesis in Three-Dimensional Scaffolds 951-963. [CrossRef]
39. D.F. Coutinho, M.E. Gomes, R.L. ReisNanomaterials for engineering vascularized tissues 229-246. [CrossRef]
40. L. L. Y. Chiu, M. Montgomery, Y. Liang, H. Liu, M. Radisic. 2012. Perfusable branching microvessel bed for vascularization of engineered tissues. *Proceedings of the National Academy of Sciences* **109**, E3414-E3423. [CrossRef]
41. Laura SuggsVascular Tissue Engineering 1-16. [CrossRef]
42. H. Perez-Hernandez, T. Paumer, T. Pompe, C. Werner, A. F. Lasagni. 2012. Contactless Laser-Assisted Patterning of Surfaces for Bio-Adhesive Microarrays. *Biointerphases* **7**, 1-9. [CrossRef]
43. Mehdi Nikkhah, Nouran Eshak, Pinar Zorlutuna, Nasim Annabi, Marco Castello, Keekyoung Kim, Alireza Dolatshahi-Pirouz, Faramarz Edalat, Hojae Bae, Yunzhi Yang, Ali Khademhosseini. 2012. Directed endothelial cell morphogenesis in micropatterned gelatin methacrylate hydrogels. *Biomaterials* **33**, 9009-9018. [CrossRef]
44. Dany J. Munoz-Pinto, Xin Qu, Loveleena Bansal, Heather N. Hayenga, Juergen Hahn, Mariah S. Hahn. 2012. Relative impact of form-induced stress vs. uniaxial alignment on multipotent stem cell myogenesis. *Acta Biomaterialia* **8**, 3974-3981. [CrossRef]
45. Lonnissa H. Nguyen, Nasim Annabi, Mehdi Nikkhah, Hojae Bae, Loïc Binan, Sangwon Park, Yunqing Kang, Yunzhi Yang, Ali Khademhosseini. 2012. Vascularized Bone Tissue Engineering: Approaches for Potential Improvement. *Tissue Engineering Part B: Reviews* **18**:5, 363-382. [Abstract] [Full Text HTML] [Full Text PDF] [Full Text PDF with Links]

46. Hwan Hee Oh, Young-Gwang Ko, Hongxu Lu, Naoki Kawazoe, Guoping Chen. 2012. Preparation of Porous Collagen Scaffolds with Micropatterned Structures. *Advanced Materials* **24**:10.1002/adma.v24.31, 4311-4316. [CrossRef]
47. Sathyanarayana Janardhanan, Martha O. Wang, John P. Fisher. 2012. Coculture Strategies in Bone Tissue Engineering: The Impact of Culture Conditions on Pluripotent Stem Cell Populations. *Tissue Engineering Part B: Reviews* **18**:4, 312-321. [Abstract] [Full Text HTML] [Full Text PDF] [Full Text PDF with Links]
48. Sonja Sokic, Georgia Papavasiliou. 2012. FGF-1 and proteolytically mediated cleavage site presentation influence three-dimensional fibroblast invasion in biomimetic PEGDA hydrogels. *Acta Biomaterialia* **8**, 2213-2222. [CrossRef]
49. Anna K. Blakney, Mark D. Swartzlander, Stephanie J. Bryant. 2012. Student award winner in the undergraduate category for the society of biomaterials 9th World Biomaterials Congress, Chengdu, China, June 1-5, 2012. *Journal of Biomedical Materials Research Part A* **100A**:10.1002/jbm.a.v100a.6, 1375-1386. [CrossRef]
50. Dhaval Patel, Susan E. Vandromme, Michael E. Reid, Lakeshia J. Taite. 2012. Synergistic Activity of α v β 3 Integrins and the Elastin Binding Protein Enhance Cell-Matrix Interactions on Bioactive Hydrogel Surfaces. *Biomacromolecules* **13**, 1420-1428. [CrossRef]
51. Hwan Hee Oh, Hongxu Lu, Naoki Kawazoe, Guoping Chen. 2012. Differentiation of PC12 cells in three-dimensional collagen sponges with micropatterned nerve growth factor. *Biotechnology Progress* **28**, 773-779. [CrossRef]
52. Pinar Zorlutuna, Nasim Annabi, Gulden Camci-Unal, Mehdi Nikkhah, Jae Min Cha, Jason W. Nichol, Amir Manbachi, Hojae Bae, Shaochen Chen, Ali Khademhosseini. 2012. Microfabricated Biomaterials for Engineering 3D Tissues. *Advanced Materials* **24**:10.1002/adma.v24.14, 1782-1804. [CrossRef]
53. Rodney T. Chen, Silvia Marchesan, Richard A. Evans, Katie E. Styan, Georgina K. Such, Almar Postma, Keith M. McLean, Benjamin W. Muir, Frank Caruso. 2012. Photoinitiated Alkyne–Azide Click and Radical Cross-Linking Reactions for the Patterning of PEG Hydrogels. *Biomacromolecules* **13**, 889-895. [CrossRef]
54. Sunny S. Shah, Mihye Kim, Elena Foster, Tam Vu, Dipali Patel, Li-Jung Chen, Stanislav V. Verkhoturov, Emile Schweikert, Giyoong Tae, Alexander Revzin. 2012. Electrochemical release of hepatocyte-on-hydrogel microstructures from ITO substrates. *Analytical and Bioanalytical Chemistry* **402**, 1847-1856. [CrossRef]
55. Hongkwan Cho, Swathi Balaji, Abdul Q. Sheikh, Jennifer R. Hurley, Ye F. Tian, Joel H. Collier, Timothy M. Crombleholme, Daria A. Narmoneva. 2012. Regulation of endothelial cell activation and angiogenesis by injectable peptide nanofibers. *Acta Biomaterialia* **8**, 154-164. [CrossRef]
56. Irza Sukmana. 2012. Microvascular Guidance: A Challenge to Support the Development of Vascularised Tissue Engineering Construct. *The Scientific World Journal* **2012**, 1-10. [CrossRef]
57. Mark A. Scott, Zachary D. Wissner-Gross, Mehmet Fatih Yanik. 2012. Ultra-rapid laser protein micropatterning: screening for directed polarization of single neurons. *Lab on a Chip* **12**, 2265. [CrossRef]
58. Matthew E. Hyndman, Deborah Kaye, Nicholas C. Field, Keith A. Lawson, Norm D. Smith, Gary D. Steinberg, Mark P. Schoenberg, Trinity J. Bivalacqua. 2012. The Use of Regenerative Medicine in the Management of Invasive Bladder Cancer. *Advances in Urology* **2012**, 1-7. [CrossRef]
59. Michael V. Turturro, Georgia Papavasiliou. 2012. Generation of Mechanical and Biofunctional Gradients in PEG Diacrylate Hydrogels by Perfusion-Based Frontal Photopolymerization. *Journal of Biomaterials Science, Polymer Edition* **23**, 917-939. [CrossRef]
60. Colette Shen, Christopher ChenRegulation of Capillary Morphogenesis by the Adhesive and Mechanical Microenvironment 165-192. [CrossRef]
61. Lucie Bacakova, Elena Filova, Martin Parizek, Tomas Ruml, Vaclav Svorcik. 2011. Modulation of cell adhesion, proliferation and differentiation on materials designed for body implants. *Biotechnology Advances* **29**, 739-767. [CrossRef]
62. Deirdre E. J. Anderson, Monica T. Hinds. 2011. Endothelial Cell Micropatterning: Methods, Effects, and Applications. *Annals of Biomedical Engineering* **39**, 2329-2345. [CrossRef]
63. J. S. Stephens-Altus, P. Sundelacruz, M. L. Rowland, J. L. West. 2011. Development of bioactive photocrosslinkable fibrous hydrogels. *Journal of Biomedical Materials Research Part A* **98A**:10.1002/jbm.a.v98a.2, 167-176. [CrossRef]
64. Chandramouleeswaran Subramani, Nergiz Cengiz, Krishnendu Saha, Tugce Nihal Gevrek, Xi Yu, Youngdo Jeong, Avinash Bajaj, Amitav Sanyal, Vincent M. Rotello. 2011. Direct Fabrication of Functional and Biofunctional Nanostructures Through Reactive Imprinting. *Advanced Materials* **23**:10.1002/adma.v23.28, 3165-3169. [CrossRef]
65. Bret D. Ulery, Lakshmi S. Nair, Cato T. Laurencin. 2011. Biomedical applications of biodegradable polymers. *Journal of Polymer Science Part B: Polymer Physics* **49**, 832-864. [CrossRef]

66. Thomas H. Barker. 2011. The role of ECM proteins and protein fragments in guiding cell behavior in regenerative medicine. *Biomaterials* **32**, 4211-4214. [CrossRef]

67. Esther C. Novosel, Claudia Kleinhans, Petra J. Kluger. 2011. Vascularization is the key challenge in tissue engineering. *Advanced Drug Delivery Reviews* **63**, 300-311. [CrossRef]

68. A. Ovsianikov, M. Malinauskas, S. Schlie, B. Chichkov, S. Gittard, R. Narayan, M. Löbler, K. Sternberg, K.-P. Schmitz, A. Haverich. 2011. Three-dimensional laser micro- and nano-structuring of acrylated poly(ethylene glycol) materials and evaluation of their cytoxicity for tissue engineering applications. *Acta Biomaterialia* **7**, 967-974. [CrossRef]

69. Laura E. Dickinson, Sravanti Kusuma, Sharon Gerecht. 2011. Reconstructing the Differentiation Niche of Embryonic Stem Cells Using Biomaterials. *Macromolecular Bioscience* **11**:10.1002/mabi.v11.1, 36-49. [CrossRef]

70. Julia E. Leslie-Barbick, Colette Shen, Christopher Chen, Jennifer L. West. 2011. Micron-Scale Spatially Patterned, Covalently Immobilized Vascular Endothelial Growth Factor on Hydrogels Accelerates Endothelial Tubulogenesis and Increases Cellular Angiogenic Responses. *Tissue Engineering Part A* **17**:1-2, 221-229. [Abstract] [Full Text HTML] [Full Text PDF] [Full Text PDF with Links]

71. B. Joddar, A.L. Sieminski, C.J. Tennant, K.J. GoochBiomaterials and the Microvasculature 35-50. [CrossRef]

72. Justin M. Saul, David F. WilliamsHydrogels in Regenerative Medicine 279-302. [CrossRef]

73. Melissa K. McHale, Nicole M. Bergmann, Jennifer L. WestHistogenesis in Three-dimensional Scaffolds 675-691. [CrossRef]

74. Justin M. Saul, David F. WilliamsHydrogels in Regenerative Medicine 637-661. [CrossRef]

75. G.B. McGuinness, N.E. Vrana, Y. LiuProcessing and fabrication technologies for biomedical hydrogels 63-80. [CrossRef]

76. Sunny Satish Shah, Mihye Kim, Katelyn Cahill-Thompson, Giyoong Tae, Alexander Revzin. 2011. Micropatterning of bioactive heparin-based hydrogels. *Soft Matter* **7**, 3133-3140. [CrossRef]

77. Yu-Chieh Chiu, Jeffery C. Larson, Anthony Isom , Jr., Eric M. Brey. 2010. Generation of Porous Poly(Ethylene Glycol) Hydrogels by Salt Leaching. *Tissue Engineering Part C: Methods* **16**:5, 905-912. [Abstract] [Full Text HTML] [Full Text PDF] [Full Text PDF with Links] [Supplemental Material]

78. Edward A Phelps, Andrés J García. 2010. Engineering more than a cell: vascularization strategies in tissue engineering. *Current Opinion in Biotechnology* **21**, 704-709. [CrossRef]

79. M A Kotlarchyk, E L Botvinick, A J Putnam. 2010. Characterization of hydrogel microstructure using laser tweezers particle tracking and confocal reflection imaging. *Journal of Physics: Condensed Matter* **22**, 194121. [CrossRef]

80. Jordan S. Miller, Colette J. Shen, Wesley R. Legant, Jan D. Baranski, Brandon L. Blakely, Christopher S. Chen. 2010. Bioactive hydrogels made from step-growth derived PEG–peptide macromers. *Biomaterials* **31**, 3736-3743. [CrossRef]

81. Shaun D Gittard, Aleksandr Ovsianikov, Boris N Chichkov, Anand Doraiswamy, Roger J Narayan. 2010. Two-photon polymerization of microneedles for transdermal drug delivery. *Expert Opinion on Drug Delivery* **7**, 513-533. [CrossRef]

82. Shaun D. Gittard, Aleksandr Ovsianikov, Hasan Akar, Boris Chichkov, Nancy A. Monteiro-Riviere, Shane Stafslien, Bret Chisholm, Chun-Che Shin, Chun-Ming Shih, Shing-Jong Lin, Yea-Yang Su, Roger J. Narayan. 2010. Two Photon Polymerization-Micromolding of Polyethylene Glycol-Gentamicin Sulfate Microneedles. *Advanced Engineering Materials* NA-NA. [CrossRef]

83. E. A. Phelps, N. Landazuri, P. M. Thule, W. R. Taylor, A. J. Garcia. 2010. Bioartificial matrices for therapeutic vascularization. *Proceedings of the National Academy of Sciences* **107**, 3323-3328. [CrossRef]

84. Preface xv-xix. [Citation] [Full Text PDF] [Full Text PDF with Links]

85. Preface xv-xix. [Citation] [Full Text PDF] [Full Text PDF with Links]

86. Ruchi Sharma, Sebastian Greenhough, Claire N. Medine, David C. Hay. 2010. Three-Dimensional Culture of Human Embryonic Stem Cell Derived Hepatic Endoderm and Its Role in Bioartificial Liver Construction. *Journal of Biomedicine and Biotechnology* **2010**, 1-12. [CrossRef]

87. Laura E. Dickinson, Matthew E. Moura, Sharon Gerecht. 2010. Guiding endothelial progenitor cell tube formation using patterned fibronectin surfaces. *Soft Matter* **6**, 5109. [CrossRef]

88. Wande Zhang, Li-Hsin Han, Shaochen Chen. 2010. Integrated Two-Photon Polymerization With Nanoimprinting for Direct Digital Nanomanufacturing. *Journal of Manufacturing Science and Engineering* **132**, 030907. [CrossRef]

89. Matthias W. Laschke, Brigitte Vollmar, Michael D. Menger. 2009. Inosculation: Connecting the Life-Sustaining Pipelines. *Tissue Engineering Part B: Reviews* **15**:4, 455-465. [Abstract] [Full Text HTML] [Full Text PDF] [Full Text PDF with Links]